Proceedings of the 23rd American Solar Energy Society Annual Conference, San Jose, CA, June 1994

UPDATED TRANSMITTANCE FUNCTIONS FOR USE IN FAST SPECTRAL DIRECT BEAM IRRADIANCE MODELS

C. Gueymard
Florida Solar Energy Center
300 State Road 401
Cape Canaveral, FL 32920

ABSTRACT

New spectral transmittance functions are introduced for the main extinction processes in the atmosphere for shortwave direct beam radiation: Rayleigh scattering, aerosol extinction, and absorption by ozone, uniformly mixed gases, water vapor, and NO_2. The latter extinction effect (in the UV and visible) is introduced for the first time in a simple spectral model. Along with an improved extraterrestrial solar spectrum at 1 nm intervals below 1700 nm, these functions constitute a spectral radiation model called SMARTS2. It can be easily compared to measured data when using its circumsolar correction and smoothing functions. A preview of broadband applications of this new model is also provided, through the derivation of improved estimates of the luminous efficacy used in daylighting calculations.

1. INTRODUCTION

Spectral solar irradiance models are needed in a variety of applications spread among different disciplines such as atmospheric sciences, biological sciences and energy technologies (PV systems, high performance glazings, daylighting, selective coatings, etc.). Two types of spectral irradiance models may be used to predict or analyze solar radiation at the Earth's surface: sophisticated rigorous codes and simple transmittance parameterizations. A well known example of the first kind is the LOWTRAN family, which originated more than 20 years ago. It has been recently supplanted by an even more detailed code called MODTRAN [1]. Such a model considers that the atmosphere is constituted of different layers, and uses reference or measured vertical profiles for its gaseous and aerosol constituents.

Because of the detailed inputs needed, execution time, and some output limitations, MODTRAN is not an appropriate code for all applications, particularly in engineering. Most of the latter needs are presently fulfilled by parameterized models which are relatively simple compared to MODTRAN. Most of the simple models that have appeared in the literature since the early '80s [2-8] are based on Leckner's landmark contribution [9]. For computerized calculations, SPCTRAL2 [10], based on [2, 3], and SUNSPEC [11], based on [5], are frequently used. (SUNSPEC is being revised in accordance with the algorithms presented here.) They are both based on Leckner's functions, at least for the determination of water vapor, mixed gases, and ozone absorptances. Much fundamental knowledge on gaseous absorption has been added since Leckner's contribution, so that a detailed reexamination of his approach appears now justified. Furthermore, data of higher spectral resolution is now available, improving accuracy in those spectral regions where gaseous absorption changes rapidly, as will be shown.

This paper will present SMARTS2, an extensive revision of the algorithms used to calculate direct beam radiation with SMARTS, a spectral model that was presented recently [5]. In short, the main objectives and achievements of this study are:

- Introduce new transmittance functions for all the atmospheric extinction processes
- Add nitrogen dioxide (NO_2) to the list of absorbers, for the first time in this type of model
- Derive very accurate absorption coefficients from recent spectroscopic data
- Improve the spectral resolution of calculations
- Improve the extraterrestrial spectrum
- Add the capability to estimate the circumsolar enhancement factor for comparison with pyrheliometric data
- Add the flexibility to smooth the output data using a Gaussian filter function.

Because of the complexity of its algorithms and space limitation, only an outline of the derivation will be given, as well as limited comparisons with MODTRAN2 and experimental data to assess its performance. Details of the derivation of SMARTS2 may be found in [12]. Finally, an application of this model in daylighting calculations is outlined in Section 7, while other applications are detailed in [13].

2. MODEL STRUCTURE AND SOLAR SPECTRUM

Under cloudless sky conditions, direct beam radiation constitutes the major part of the incoming shortwave radiation. Moreover, its measurement can be used to derive information on atmospheric conditions (e.g., gaseous abundance and turbidity) by comparison with model calculations run backwards. (Such a technique based on the present work is being developed [14].) For these reasons, all that follows is concerned with direct beam radiation. However, SMARTS2 also has provision to calculate diffuse radiation on a horizontal or tilted plane, using the methodology described in [12].

The beam irradiance received at ground level by a surface normal to the sun rays (or "beam normal irradiance") at wavelength λ is given by:

$$E_{bn\lambda} = E_{on\lambda}\, T_{R\lambda}\, T_{a\lambda}\, T_{g\lambda}\, T_{o\lambda}\, T_{n\lambda}\, T_{w\lambda} \qquad (1)$$

where $E_{on\lambda}$ is the extraterrestrial irradiance corrected for the actual sun-earth distance and the other terms are the transmittances for the different extinction processes considered here: Rayleigh scattering, aerosol extinction, and absorption by uniformly mixed gases, ozone, NO_2, and water vapor, respectively. Note that NO_2 absorption in the UV and visible is introduced here for the first time in a simple spectral irradiance model. It is not even considered yet in MODTRAN2. (The latest version used here was kindly provided in August 1993 by Jim Chetwynd, Phillips Lab.)

Whereas SMARTS1 used the WRC85 spectrum [15], SMARTS2 uses a slightly modified spectrum, at 1 nm intervals between 280 and 1700 nm, and at 5 nm intervals between 1700 and 4000 nm. The total irradiance is 1350.0 W/m^2, compared to 1349.5 W/m^2 for the WRC85 spectrum, for a solar constant of 1367 W/m^2. This new spectrum is justified because (i) Some problems were discovered in the WRC85 spectrum, including an anomalous dip in the 920-980 nm range [personal communications with Claus Fröhlich, 1992, and Eric P. Shettle, 1993]; (ii) New high altitude balloon and satellite data have been published recently, particularly in the UV. The new spectrum has a total of 1881 wavelengths, compared to 545 wavelengths for the spectrum used in SMARTS1 and 122 wavelengths used in SPCTRAL2. This certainly gives a rather high resolution for engineering use, but the model output (transmittances and irradiance) can be downgraded afterwards according to the user's needs (see Section 5).

The different optical masses, which play a key role in the transmittance functions, have already been described [5, 16].

3. INDIVIDUAL TRANSMITTANCES

• ***Rayleigh scattering:*** The Rayleigh optical depth has been recalculated from its theoretical expression, using Young's determination of the depolarization factor [17] and Peck & Reeder's formula [18] for the spectral variation of the refractive index. A least-squares curve fitting technique was used to develop the following equation:

$$T_{R\lambda} = \exp[-m_R\, P / (a_1\, \lambda^4 + a_2\, \lambda^2 + a_3 + a_4\, \lambda^{-2})] \qquad (2)$$

where m_R is the optical air mass, P is the ratio of the site pressure to the standard value (1013.25 mb), a_1= 117.2594, a_2=-1.3215, a_3=3.2073E-4 and a_4=-7.6842E-5. Eqn. (2) fits the basic spectral calculations with an average deviation of less than 0.01%.

• ***Ozone absorption:*** The Bouguer law is used to describe ozone absorption, i.e.

$$T_{o\lambda} = \exp(-m_o\, u_o\, A_{o\lambda}) \qquad (3)$$

where m_o is the ozone optical mass, u_o its reduced pathlength (in atm-cm), and $A_{o\lambda}$ its spectral absorption coefficient.

Ozone absorbs strongly in the UV, moderately in the visible, and slightly in the near infrared. In the UV (Hartley-Huggins bands), recent spectroscopic data [19-21] were smoothed to 1 nm resolution for the region 280–365 nm. The basic absorption coefficients are for a reference temperature of 228 K and a temperature correction is applied (if λ<344 nm) for other temperatures. The estimated atmospheric ozone temperature is obtained from a weighted average of the concentration and temperature profiles defined in tabulated reference atmospheres [22]. This results in an average ozone temperature of 213 to 235.7 K. To approach actual conditions at any site and time, a seasonal correlation with the screen-level air temperature, t_a, is considered.

In the visible and near infrared (Chappuis and Wulf bands, 407 to 1091 nm), the recent data in [23, 24] were downgraded to 1 nm intervals, from a dataset that will be used in future versions of MODTRAN [personal communication with Eric P. Shettle, 1994]. A temperature dependence is considered between 407 and 560 nm as above.

Finally, some absorption is present above 3120 nm. The corresponding absorption coefficients were obtained by smoothing MODTRAN2 transmittance results at 5 nm intervals.

• ***Nitrogen dioxide absorption:*** NO_2 transmittance is modelled similar to ozone, i.e.,

$$T_{n\lambda} = \exp(-m_n\, u_n\, A_{n\lambda}) \quad (4)$$

where m_n is the NO_2 optical mass, u_n its reduced pathlength (in atm-cm), and $A_{n\lambda}$ its spectral absorption coefficient. NO_2 is a highly variable atmospheric constituent that plays a key role in the ozone cycle, both in the troposphere (where its concentration may be high due to pollution) and in the stratosphere. Total column measurements in an industrial city resulted in widespread values of u_n, ranging from 4.4E-5 to 1.3E-2 atm-cm [25]. It is most probable that low NO_2 concentrations correspond to a predominant stratospheric loading at the ozone layer altitude, whereas high NO_2 concentrations are associated with tropospheric man-made pollution. Because of this layer splitting, m_n is calculated as a weighted mean of m_o and m_w, the water vapor optical mass.

The values of $A_{n\lambda}$ were derived from data in [26, 27] in the 280 to 700 nm range and smoothed to 1 nm intervals. As with ozone, a temperature dependence is considered. Because of the variations in the balance between stratospheric and tropospheric NO_2, its average atmospheric temperature is defined as a weighted mean between the ozone temperature defined earlier and t_a.

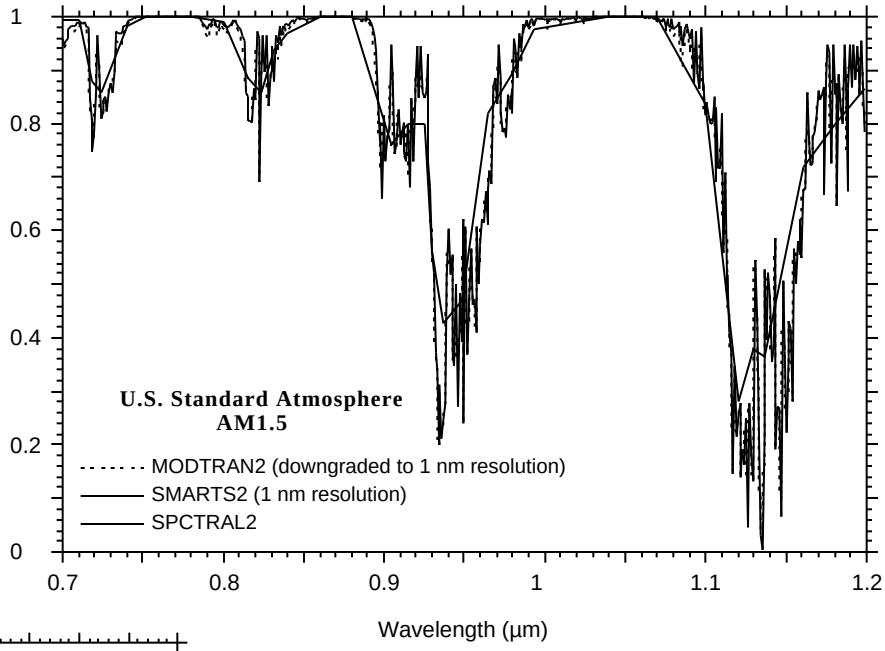

Fig. 2 Water vapor transmittance for U.S. Standard Atmosphere (w=1.419 cm) at air mass 1.5.

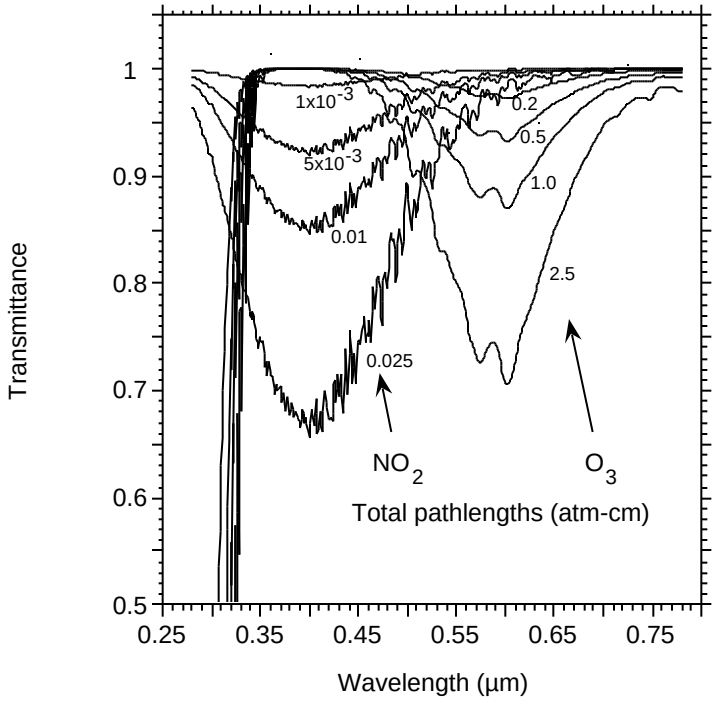

Fig. 1 Ozone and NO_2 transmittances for different total pathlengths ($m_o u_o$ and $m_n u_n$, resp.)

The transmittances for O_3 and NO_2 are compared in Fig. 1 for different total pathlengths, $m_o u_o$ and $m_n u_n$, respectively. These transmittances are almost equivalent when $m_n u_n$ is about a factor of 100 less than $m_o u_o$.

• ***Uniformly mixed gases:*** Some atmospheric constituents (principally O_2 and CO_2) have a monotonically decreasing atmospheric concentration with altitude and significant absorption bands in the infrared. Based on the analysis in [28, 29], the corresponding transmittance is defined as:

$$T_{g\lambda} = \exp[-(m_g\, u_g\, A_{g\lambda})^a\, P^b] \quad (5)$$

where $m_g = m_R$ is the optical air mass, u_g the gaseous pathlength (about 5 km), and $A_{g\lambda}$ the spectral absorption coefficient. The exponent a was obtained by fitting data in [28, 29] such that $a = 0.5641$ for $\lambda < 1000$ nm, or else $a = 0.7070$. The exponent b was obtained as 1.14, by analyzing different MODTRAN2 runs for different altitudes (up to 4 km). The values of $A_{g\lambda}$ were also obtained by smoothing MODTRAN2 transmittance results for different reference atmospheres, and reversing eqn. (5).

• ***Water vapor absorption:*** In the spectral range considered here, water vapor is by far the most important absorber. The accurate determination of its transmittance is therefore most important in a radiation model. A new functional form has been derived based on the one used in SMARTS1 [5] for a part of the near infrared region, and on the one proposed in [30]:

$$T_{w\lambda} = \exp\{-[(m_w\, w)^c\, f_w{}^n\, A_{w\lambda}]^{1.5}\} \quad (6)$$

where m_w is the water vapor optical mass, w the total precipitable water (in cm), f_w a scaling factor (a function of λ and t_a) accounting for the inhomogeneity of the water vapor pathlength, and c and n are wavelength-dependent exponents (obtained by fitting data in [30]). Precipitable water, w, can be obtained by different experimental methods or by using empirical relationships between w and the screen-level temperature and humidity (e.g., [9, 31]).

The values of $A_{w\lambda}$ were obtained the same way as $A_{g\lambda}$ previously, i.e., from MODTRAN2 results (including the continuum absorption effects). It is important to note that MODTRAN2 absorption calculations are themselves based on HITRAN'92, the latest edition of a high resolution spectroscopic atlas.

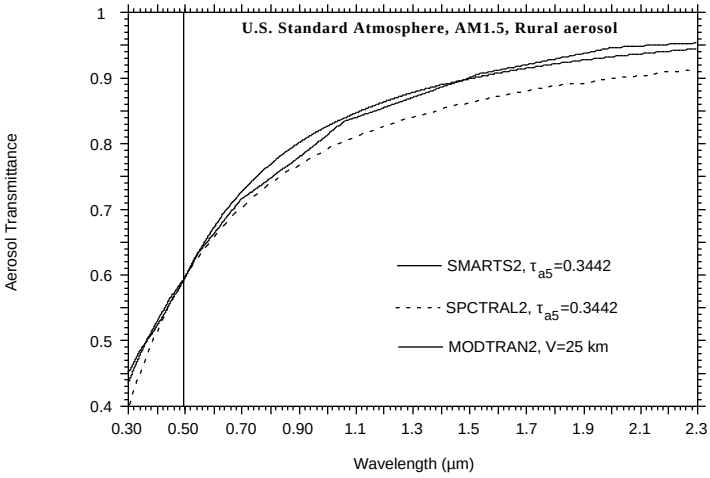

Fig. 3 SMARTS2, MODTRAN2 and SPCTRAL2 aerosol transmittances for equivalent turbidity conditions

Figure 2 displays the water vapor transmittance in the 940 nm band as calculated by SMARTS2, MODTRAN2, and SPCTRAL2 for the U.S. Standard Atmosphere (w=1.419 cm) and an air mass of 1.5 (corresponding to the ASTM standardized conditions [32]). The difference between the predictions of SMARTS2 and MODTRAN2 is virtually indiscernible, whereas SPCTRAL2 is off by a significant margin in some wavelength intervals, due to its crude resolution and older absorption data.

• ***Aerosol extinction:*** Spectral optical characteristics of the tropospheric and stratospheric aerosols change rapidly with time and with meteorological conditions. Although spectral determinations of the aerosol optical thickness would be needed, such measurements are rare, so that only broad climatological information is available in the general case, if at all.

A simplified methodology, using the same modified Angström approach as in SMARTS1 [5], is therefore justified. Turbidity may be expressed in terms of three possible coefficients: $ß$ (defined at 1000 nm), τ_{a5} or B (defined at λ_0=500 nm), and turbidity exponents α_1 (for $\lambda<\lambda_0$) and α_2 (for $\lambda>\lambda_0$). The aerosol transmittance is then obtained as:

$$T_{a\lambda} = \exp[-m_a\, ß\, q\, (\lambda/\lambda_0)^{-\alpha}] \quad (7)$$

where $m_a = m_w$ is the aerosol optical mass, $\alpha=\alpha_1$ if $\lambda<\lambda_0$ and α_2 otherwise, and $q=2^{\alpha 2-\alpha 1}$ if $\lambda<\lambda_0$ and q=1 otherwise. The correspondence between $ß$, τ_{a5} and B results from their respective definitions and is mentioned in [5].

Typical values of coefficients α_1 and α_2 have been obtained by linearly fitting the spectral aerosol coefficients of four aerosol types used in MODTRAN [33] for relative humidities between 0 and 99% (Table 1). As it clearly shows, α_1 is always less than α_2, both α_1 and α_2 tend to decrease when relative humidity increases, and the average ratio α_1/α_2 is close to 0.7 for the rural, urban, and maritime aerosols at relative humidities ≤70%.

Figure 3 presents a comparison of the aerosol transmittance as predicted by SMARTS2, MODTRAN2, and SPCTRAL2. The latter uses a function simpler than eqn. (7), because it considers $\alpha_1=\alpha_2$=1.14. Both SMARTS2 and SPCTRAL2 have been used with τ_{a5}=0.3442, corresponding to a visual range, V, of 25 km in MODTRAN2. It should be noted that the ASTM standard [32] is based on τ_{a5}=0.27, which corresponds to V=25 km according to [34] — or incorrectly, 23 km according to [32]. The correspondence between V=25 km and τ_{a5}=0.27 is only exact when using the outdated aerosol data found in LOWTRAN4 or older versions.

TABLE 1 Turbidity exponents for different aerosol types

Humidity		0%	50%	70%	90%	99%
Rural	α_1	0.933	0.932	0.928	0.844	0.659
	α_2	1.444	1.441	1.428	1.377	1.134
Urban	α_1	0.822	0.827	0.838	0.779	0.492
	α_2	1.167	1.171	1.186	1.256	1.127
Maritime	α_1	0.468	0.449	0.378	0.232	0.107
	α_2	0.626	0.598	0.508	0.246	0.053
Tropospheric	α_1	1.010	1.008	1.005	0.911	0.797
	α_2	2.389	2.379	2.357	2.130	1.962

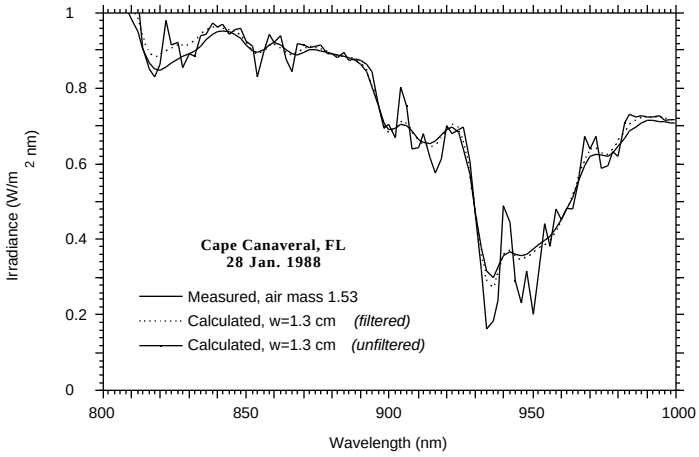

Fig. 4 Measured irradiance vs filtered and unfiltered SMARTS2 predictions for a the 940 nm water vapor band

4. CIRCUMSOLAR RADIATION

The direct beam radiation calculated so far ideally comes from the solar disk only. When comparing such data to actual measured data, it is important to add the circumsolar diffuse radiation that is also intercepted in the aperture (e.g., 5.7°) of an actual pyrheliometer. This circumsolar contribution increases with turbidity and optical mass. Theoretical calculations are underway to derive an accurate spectral correction function. In the mean time, a broadband correction factor [35] is used equally at all wavelengths. This factor is only dependent on the product ($m_a ß$) but implicitly assumes that α_2 is about 1.3. For different values of α_2, $ß$ can be corrected by assuming that the representative wavelength for the circumsolar radiation is λ_p=555 nm (the peak of the photopic curve), which is close and about halfway between the peak of the diffuse spectrum and its median. It is therefore proposed to replace $ß$ in eqn. (28) of [35] by $ß\,\lambda_p^{\alpha 2-1.3}$.

5. OUTPUT DATA SMOOTHING

Spectroradiometric instruments possess differing spectral bandpass widths and shapes. The Gaussian and triangular shapes were chosen here as representative. A new feature of SMARTS2 is a post-processor that scans the raw output and smooths it to derive new outputs at possibly wider intervals (depending on the user's needs), approximating the instrumental transmittance characteristics by a Gaussian or triangular function with a known FWHM (full width at half maximum).

6. COMPARISON WITH MEASURED DATA

Detailed comparison against carefully measured data is a good way to assess the performance of a model. An example of such a comparison will be provided here, using the dataset measured at the Florida Solar Energy Center under the auspices of the National Renewable Energy Laboratory. A temperature controlled LiCor LI-1800 spectroradiometer sampled the spectrum between 300 and 1100 nm at 2 nm intervals. The instrumental FWHM was 6.15 nm. The other experimental conditions are detailed in [36].

Figure 4 presents a comparison in the near infrared between measured and calculated data for cloudless conditions at an air mass of 1.53. Modelled data were either plotted at every other wavelength (to approximate the 2 nm increment of the measured data) or smoothed first, using the methodology of Section 5, to match the instrumental characteristics. It is clear from Fig. 4 that a preliminary smoothing processs is essential to make qualitatively and quantitatively correct comparisons. It appears also that SMARTS2 closely follows the intricacies of the water vapor absorption features which were recorded.

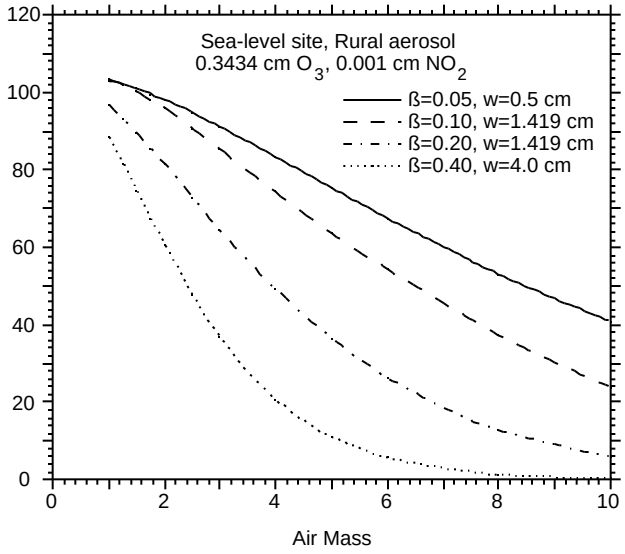

Fig. 5 Luminous efficacy as a function of air mass for different atmospheric conditions

7. APPLICATION TO DAYLIGHTING

Once accurate transmittance functions have been developed, it is possible to perform a spectral integration in order to obtain an average transmittance within a specified spectral range or even within the entire broadband shortwave spectrum. An example of this application, concerning daylighting, is outlined here. Illuminance data are needed to correctly design buildings for daylighting. Because spectral measurements are scarce, it is customary to use broadband irradiance data and to apply a correction factor, the luminous efficacy, to obtain illuminance. In the present work, the beam illuminance has been obtained directly from the spectral beam irradiance using the method

described in [5]. The luminous efficacy (in lm/W) is then found as the ratio between illuminance (in lux) and the broadband irradiance (in W/m^2) between the SMARTS2 limits of 280 and 4000 nm. The luminous efficacy for beam radiation is plotted in Fig. 5 as a function of air mass for different atmospheric conditions. It shows that air mass, precipitable water, and turbidity have a strong and complex influence on the efficacy, which would be difficult to analyze systematically from experimental data alone.

8. CONCLUSION

The new spectral transmittance functions presented here closely fit the most recent extinction data available. They can be used to approximate the predictions of a rigorous code (MODTRAN2), or to simulate measured spectroradiometric data. Future work will be devoted to the use of this new model in various spectral and broadband applications for which a preview has been presented.

9. ACKNOWLEDGEMENTS

The author is particularly thankful to all individuals who contributed largely to this work by providing basic data or valuable discussions: Len Abreu, Gail P. Anderson, Chris A. Cantrell, James H. Chetwynd, Dominique Daumont, L. A. Hall, Michael E. van Hoosier, Paul Jindra, Ross McCluney, Eric P. Shettle, and David E. Soule. This work was partially funded by grant DE-FG01-90CE21048 from the Office of Building Technologies, U.S. Department of Energy.

10. REFERENCES

1. A. Berk, et al., *MODTRAN: A moderate resolution model for LOWTRAN7*. Air Force Geophysical Lab., Hanscom, MA, Rep. GL-TR-89-0122 (1989).

2. R. E. Bird, *Solar Energy*, **32**: 461-471 (1984).

3. R. E. Bird and C. Riordan, *J. Clim. Appl. Meteor.*, **25**: 87-97 (1986).

4. D. T. Brine and M. Iqbal, *Solar Energy*, **30**: 447-453 (1983).

5. C. Gueymard, Development and performance assessment of a clear sky spectral radiation model. Proc. Solar '93—22nd ASES Conf.: 433-438 (1993).

6. C. G. Justus and M. V. Paris, *J. Clim. Appl. Meteor.*, **24**: 193-205 (1985).

7. L. K. Matthews et al., Measurement and analysis of solar spectral irradiance. Proc. ASME/JSME/JSES Solar Eng. Conf.: 307-313 (1987).

8. S. Nann and C. Riordan, *J. Appl. Meteorol.*, **30**: 447-462 (1991).

9. B. Leckner, *Solar Energy*, **20**: 143-150 (1978).

10. C. Riordan, *SPCTRAL2, FORTRAN computer program.* National Renewable Energy Lab., Golden, CO (1990).

11. R. McCluney and C. Gueymard, *Sunspec 1.0.* Florida Solar Energy Center, Rep. FSEC-SW-3-93 (1993).

12. C. Gueymard, *Simple Model of the Atmospheric Radiative Transfer of Sunshine, version 2 (SMARTS2): Algorithms description and performance assessment.* Florida Solar Energy Center, Rep. FSEC-PF-270-94 (1994).

13. C. Gueymard, *Cloudless solar irradiance models for different bands of the shortwave solar spectrum.* Florida Solar Energy Center, Rep. FSEC-PF-271-94 (1994).

14. D. E. Soule et al., Relation of aerosol optical depth to visibility and its influence on spectral solar irradiance. Manuscript in preparation (1994).

15. C. Wehrli, *Extraterrestrial solar spectrum.* World Radiation Center, Davos, Switz., Pub. No. 615 (1985).

16. C. Gueymard, *Solar Energy*, **51**: 121-138 (1993).

17. A. T. Young, *J. Appl. Meteorol.*, **20**: 328-330 (1981).

18. P. M. Teillet, *Appl. Opt.*, **29**: 1897-1900 (1990).

19. M. Cacciani, et al., *J. Geoph. Res.*, **94D**: 8485-8490 (1989).

20. D. Daumont, et al., *J. Atmos. Chem.*, **15**: 145-155 (1992).

21. L. T. Molina and M. J. Molina, *J Geoph. Res.*, **91D**: 14,501-14,508 (1986).

22. G. P. Anderson, et al., *AFGL atmospheric constituent profiles (0–120 km).* Air Force Geophysics Lab., Hanscom AFB, MA, Rep. AFGL-TR-86-0110 (1986).

23. S. M. Anderson, *Geoph. Res. Lett.*, **19**: 933-936 (1992).

24. S. M. Anderson, *Geoph. Res. Lett.*, **20**: 1579-1582 (1993).

25. R. Schroeder and J. A. Davies, *Atmosphere-Ocean*, **25**: 107-114 (1987).

26. J. A. Davidson, et al., *J. Geoph. Res.*, **93D**: 7105-7112 (1988).

27. W. Schneider, et al., *J. Photochem. Photobiol.*, **40**: 195-217 (1987).

28. J. H. Pierluissi and C. M. Tsai, *Appl. Opt.*, **25**: 2458-2460 (1986).

29. J. H. Pierluissi and C. M. Tsai, *Appl. Opt.*, **26**: 616-618 (1987).

30. J. H. Pierluissi et al., *Appl. Opt.*, **28**: 3792-3795 (1989).

31. C. Gueymard, Analysis of monthly average atmospheric precipitable water and turbidity in Canada and Northern United States, *Solar Energy* (1994, in press).

32. ASTM, *Standard tables for terrestrial direct normal solar spectral irradiance for air mass 1.5.* American Society for Testing and Materials, No. E891-87 (1987).

33. E. P. Shettle and R. W. Fenn, *Models for the aerosols of the lower atmosphere and the effects of humidity variations on their optical properties.* Air Force Geophysics Lab., Hanscom, MA, Rep. AFGL-TR-79-0214 (1979).

34. R. E. Bird et al., *Solar Energy*, **30**: 563-573 (1983).

35. C. Gueymard, *Solar Energy*, **38**: 367-386 (1987).

36. C. J. Riordan, et al., *Spectral data base documentation.* Solar Energy Research Institute, Rep. SERI/TR-215-3513 (1990).